Journal of Electroanalytical Chemistry 856 (2020) 113629

Contents lists available at ScienceDirect

Journal of Electroanalytical Chemistry

journal homepage: www.elsevier.com/locate/jelechem

Microwave-assisted synthesis of localized surface plasmon resonance enhanced bismuth selenide (Bi_2Se_3) layers for non-enzymatic glucose sensing

A. Dennyson Savariraj [a,b,*], V. Vinoth [c], R.V. Mangalaraja [a,d,**], T. Arun [e], David Contreras [f], Ali Akbari-Fakhrabadi [e], Héctor Valdés [c], Fawzi Banat [b]

[a] Advanced Ceramics and Nanotechnology Laboratory, Department of Materials Engineering, University of Concepcion, Concepcion, Chile
[b] Department of Chemical Engineering, Khalifa University of Science and Technology, Abu Dhabi, P.O. Box: 127788, United Arab Emirates
[c] Laboratorio de Tecnologías Limpias, Facultad de Ingeniería, Universidad Católica de la Santísima Concepción, Concepción, Chile
[d] Technological Development Unit (UDT), University of Concepcion, Coronel Industrial Park, Coronel, Chile
[e] Advanced Materials Laboratory, Department of Mechanical Engineering, University of Chile, Santiago, Chile
[f] Department of Analytical and Inorganic Chemistry, Faculty of Chemical Sciences, Centre for Biotechnology, University of Concepcion, Chile

ARTICLE INFO

Keywords:
Bismuth selenide
Microwave synthesis
Localized surface plasmon resonance (LSPR)

ABSTRACT

Three-dimensional (3D) bismuth selenide (Bi_2Se_3) nanostructures were synthesized by microwave synthesis using water as a solvent and hydrazine hydrate as a reducing agent and exfoliated into few layers of Bi_2Se_3. Bi_2Se_3- Few Layers (Bi_2Se_3- FL) exhibited localized surface plasmon resonance and enhanced electrocatalytic behavior. The scanning electron microscope (SEM) and transmission electron microscopy (TEM) characterization indicated the layered structure of Bi_2Se_3. The electrocatalytic properties of the Bi_2Se_3-FLmodified GC electrode towards non-enzymatic glucose oxidation were evaluated by cyclic voltammetry (CV) and chronoamperometry. The designed non-enzymatic glucose sensor showed a low detection limit of 6.1 μM, a linear range from 10 μM to 100 μM of glucose concentration and a current sensitivity of 0.112 $\mu A \mu M^{-1}$.The electrochemical sensor constructed using Bi_2Se_3-FL attained steady-state level within 3 s upon adding glucose and remained stable even after 19 days with only 17% loss in current signal. The obtained electrodes can be applied for determining glucose in urine samples. The results obtained here are of great significance to use nanostructured Bi_2Se_3-FL electrode as a potential candidate for non-enzymatic glucose detection.

1. Introduction

In human body glucose present in the blood is a vital source of energy to supply energy for the daily activities. When the glucose content in the blood exceeds requirements, the excess glucose causes diabetes mellitus, a common disease that can result in disability and death [1]. Ever since the discovery of the first enzyme based electrochemical glucose biosensor in 1962 by Clark et al., there have been constant efforts by the researchers to replace enzymatic electrochemical biosensors due its high cost, difficulty in enzyme immobilization process and decline in the activity of enzymes, irrespective of its high selectivity and sensitivity [1–3].In pursuit of identifying cost-effective catalysts for non-enzymatic glucose electro oxidation several catalysts have been reported including layered materials such as graphene [4] metal nitrides [5] and metal chalcogenides [6]. Since the transition metal based catalysts are less preferred owing to decreased specific area from close packing and poor conductivity, the non-enzymatic glucose detection mostly comprised of hybrid materials involving complex procedure and effective grafting. Therefore, careful engineering of the catalyst possessing large surface area and ample active sites along with structural stability are the prerequisites for ideal performance [7].There are several attempts on investigating the electrochemical detection of glucose using pristine forms of layered materials although bismuth selenide (Bi_2Se_3) is almost unexplored.

* Corresponding author. Advanced Ceramics and Nanotechnology Laboratory, Department of Materials Engineering, University of Concepcion, Concepcion, Chile. Tel.: +56 41 2201346; fax: +56 41 2203391.
** Corresponding author. Advanced Ceramics and Nanotechnology Laboratory, Department of Materials Engineering, University of Concepcion, Concepcion, Chile. Tel.: +56 41 2207389; fax: +56 41 2203391.
E-mail addresses: dennysons@gmail.com, dennyson.antonysamy@kustar.ac.ae (A.D. Savariraj), mangal@udec.cl (R.V. Mangalaraja).

https://doi.org/10.1016/j.jelechem.2019.113629
Received 29 July 2019; Received in revised form 21 October 2019; Accepted 4 November 2019
Available online 16 November 2019

Bi_2Se_3 is a well-known semiconducting metal chalcogenides of the V-VI groups having potential applications in optoelectronics, thermoselectronic devices and infrared spectroscopy [8]. Bi_2Se_3 is one of the layered semiconducting materials with a narrow bandgap and tetradymite structure with space group D^5_3d(R3 m). Its electronic structure with the existence of six valley degeneracy and narrow bandgap makes it suitable for optical and photosensitive device applications [9–12]. Even though Bi_2Se_3 has been synthesized in the form of nanoparticles [13], nano films [14], nanotubes [15], nanobelts [16], heterostructured nanowires [17] and layers [18] by a variety of methods [9], obtaining layered structures with high surface area to volume ratio will be desired for sensing ensuring better electrocatalytic activity.

Traditional synthesis methods do involve slow heating [19], while in microwave method the electric field supplies a force on the charged particles that makes them either to rotate or migrate and these movements result in further polarization. The electric and magnetic components of the microwaves drastically change in direction and the microwave energy provides the heat in different parts of the reaction mixture [20]. Therefore microwave heating is an advantageous synthesis technique as compared to the other conventional techniques since it supplies rapid internal volumetric heating by direct transmission with efficient and quick energy transfer into the molecules present in the reaction mixture [21]. This results in uniform increase of solution's temperature, reduced reaction time, saving of energy [22–24] and increase in the product yield [25] and rate constant as well [26]. Although significant efforts have been devoted towards the synthesis of hierarchical nanostructured bismuth selenide, most attempts involve either complicated multistep process using expensive precursors and solvents. Several works on microwave-assisted synthesis of Bi_2Se_3 with different structures and morphology such as nanoparticles [13,20] nanocrystals [13] and nanosheets [9] have been already reported in the literature.

In this report, we present a simple synthetic route to obtain layered bismuth selenide by microwave irradiation using water as a solvent. Herein we use hydrazine hydrate (N_2H_4) for its dual role, as a reducing agent and as a surfactant. The as-prepared Bi_2Se_3-Bulk (Bi_2Se_3–B) exhibits its absorption in the near-infrared (NIR) region suggesting the presence of localized surface plasmon resonance (LSPR). This phenomenon is usually found to occur in noble metals such as gold and silver, doped semiconductors or graphene where the surface-bound collective excitations of free charge carriers can involve in very strong light-matter interactions [27–29]. LSPR exists from the ultraviolet region to near-infrared and this will occur when the materials are in nanoscale due to quantum confinement that quantizes topological surface states [30]. The exfoliated Bi_2Se_3-FL possess a larger surface area than its 3D bulk counterparts (Bi_2Se_3–B). The increased surface area and high carrier density combinedly boost the electrocatalytic nature of the material. Therefore, we have attempted to investigate the LSPR enhanced nanostructured Bi_2Se_3-FL for non-enzymatic glucose sensing. In this report, highly stable and ultrasensitive non-enzymatic glucose sensor developed using Bi_2Se_3-FL nanostructures, synthesized and exfoliated by cost-effective wet-chemical route is presented. In recent years noble metals, and their oxides nitrides, hydroxides and phosphides have received intense research attention towards glucose electrooxidation due to their electro catalytic properties [1,5,7,31–33].To the best of our knowledge, glucose sensing studies for graphene like nanostructured Bi_2Se_3-FL have not been explored yet. The formation mechanism, the potential influence of 2D structure and LSPR on the resulting electrocatalytic activity have been discussed in detail. Bi_2Se_3-FL with sheet like surface offer more active sites whereby the electrochemical performance is enhanced towards the detection of glucose with pronounced stability over long period of time. The non-enzymatic glucose sensor constructed using Bi_2Se_3-FL exhibited a low detection limit of 6.1 μM and a linear range between 10 μM and 100 μM of glucose concentration with a current sensitivity of 0.112 $\mu A \mu M^{-1}$. In addition, the electrochemical sensor showed an appreciable stability beyond 19 days with a minimal loss of 17% suggesting the suitability of Bi_2Se_3-FL for non-enzymatic glucose sensing.

2. Experimental part

2.1. Materials

Bismuth nitrate pentahydrate, ($Bi(NO_3)_3{\cdot}5H_2O$), Hydrazine hydrate (N_2H_4), Selenium (Se) powder, Sodium sulfite (Na_2SO_3),Glucose, Uric acid (UA), Ascorbic acid (AA), Potassium Ferricyanide ($K_3[Fe(CN)_6]$), Sodium phosphate dibasic (Na_2HPO_4), Sodium phosphate monobasic (NaH_2PO_4), Nafion and Ethanol, were purchased from Sigma Aldrich Corporation. All chemicals were of reagent grade. Milli-Q water was used to prepare the aqueous solutions for the experiments.

2.2. Preparation of sodium selenosulfate (Na_2SeSO_3)

Since the pristine Selenium (Se) is not water-soluble and does not react efficiently in its pristine form, sodium selenosulfate (Na_2SeSO_3) was prepared using the procedures from our earlier report [34]. Solutions of 0.2 M selenium (Se) and 0.4 M of sodium sulfite (Na_2SO_3) were prepared and transferred to a round bottom flask followed by adding deionized (DI) water. This solution was refluxed for a period of 2 h at 125 °C–130 °C using an oil bath set up to obtain Na_2SeSO_3. The solution was filtered and used as Se source for the preparation of nanostructured 3D Bi_2Se_3 layers.

2.3. Material characterization

The prepared bismuth selenide was characterized by using powder X-ray diffraction (XRD) technique (Bruker, D4 Endeavor) with a diffraction angle of (2θ) in the range of 10°–90° to identify the crystalline nature of the material. X-ray photoelectron analysis was carried out using Kratos Axis Ultra DLD X-ray photoelectron spectrometer with monochromatic Al Kα (1486.708 eV) radiation. The Surface morphology was characterized using scanning electron microscope (SEM, JEOL JSM-6380 LV), CSI Nano-Observer AFM and transmission electron microscope (TEM, JEOL JEM 1200 EXII) while the optical measurements were carried out through absorption spectroscopy by using Shimadzu UV–Vis 2600 spectrometer. All electrochemical measurements were performed in a three-electrode electrochemical cell using a CHI 6044E workstation (CHI Instruments, USA). All experiments were conducted at room temperature.

2.4. Microwave synthesis of Bi_2Se_3-FL and exfoliation

0.072 M Bismuth nitrate pentahydrate ($Bi(NO_3)_3.5H_2O$) was added to a beaker containing 25 mL of DI water and stirred for 15 min. To this 25 mL of Na_2SeSO_3 solution was added in drops followed by the addition of 1mL of Hydrazine hydrate (N_2H_4). The above said reaction mixture was further stirred for 30 min and subjected to microwave irradiation for 5 min. The resultant black precipitate containing layered Bi_2Se_3 -B was centrifuged several times using DI water until neutral pH was reached followed by washing with absolute ethanol and then dried in a vacuum oven at 60 °C for 12 h.1 mg of the as-prepared Bi_2Se_3 -B was added to a vial containing 10 mL of ethanol and water mixture (3:2 v/v). The dispersion was sonicated for 4 h and centrifuged to obtain the Bi_2Se_3-FL.

2.5. Electrochemical investigation

A 10 mL glass electrochemical cell containing three electrodes was used for the electrochemical investigation. In a typical experiment a glassy carbon (GC) disk electrode was used as a working electrode (3 mm diameter) while a platinum wire, and Ag/AgCl (saturated KCl) electrodes were used as the auxiliary and reference electrodes, respectively. Prior to modification, the GC was polished with a polishing cloth, using 3.0, 1.0 and 0.05 μm alumina slurries, rinsed thoroughly with ultrapure water, and sonicated in a mixture of ethanol and water (1:1 v/v) for 5 min. 1 mg

of Bi_2Se_3–B was measured accurately and uniformly dispersed in 10 mL of ethanol water mixture and sonicated for 10 min to obtain uniform dispersion. A volume of 10 μL of Bi_2 Se_3–B solution was drop casted on previously cleaned GC and dried at room temperature to fabricate Bi_2Se_3–B/GC electrode. Similarly, 10 μL of Bi_2Se_3-FL obtained using the above said procedure was drop casted on a previously cleaned GC and dried at room temperature to fabricate Bi_2Se_3-FL/GC electrode. For real sample analysis, human urine was obtained from a healthy volunteer. The urine sample was analyzed directly without any pretreatment and was stored in the refrigerator at low temperature until the completion of all analysis. About 20 mL was centrifuged at 8000 rpm for 10 min at room temperature in order to separate the liquid in the urine from solid components such as mineral crystals, blood cells or microorganism.

3. Result and discussion

3.1. Characterization of synthesized Bi_2Se_3

Bi_2Se_3 are layered materials possessing rhombohedral crystal stratum of the space group D3d (R3m). Every layer is made of five monoatomic sheets called quintuple layer (QL) and the atoms in a sheet are covalently bonded in the order of X–Bi−X–Bi−X where X = Se or Te [18]. The phase purity and crystal structure of the as-prepared 3D Bi_2Se_3 layers were examined by powder X-ray diffraction and the respective spectrum is presented in Fig. S1. In Fig. S1 (see Supporting information), the absence of characteristic peaks corresponding to impurities suggests that the final product is highly pure with certain amount of crystalline nature. The signature peaks in the pattern ((015), (110), (0015) and (205)) can be assigned to the reflection of Bi_2Se_3 rhombohedral phase (symmetry R3m) of preferential orientation of the crystallites owing to its layered structure (a = b = 4.1396 Å, c = 28.6360Å, α = β = 90°, γ = 120°, ICDD 33–0214) [35,36].

Fig. 1 (A), shows the UV–vis absorbance spectrum of Bi_2Se_3–B, dispersed in ethanol: water (3:2) mixture at room temperature. From the spectrum, it is evident that there are three broad peaks at 296 nm, 671 nm and 789 nm. The absorption in the region beyond 900 nm provides an evidence for the presence of LSPR [35,37], which would reflect in the electrocatalytic activity of this material. The LSPR phenomenon is usually encountered in noble metals in nanoscale when they interact with light and it is characterized by surface-bound charge densities in resonance with driving magnetic field [38].Surface plasmon resonance is found in semiconductors with free carrier densities due to self-doping causing cation vacancies. These free carrier concentration are usually tuned by doping, temperature and/or phase transition [38–40].

X-Ray photoelectron spectroscopy (XPS) was carried out in order to investigate the chemical composition of the as-synthesized Bi_2Se_3–B. The full-range survey scan spectrum (Fig. 1 (B)), exhibits peaks corresponding to Bi and Se peaks confirm the presence of Bi and Se. There are also two other peaks observed corresponding to O and C indicating the presence of O and C which is due to moisture uptake and surface hydrocarbon contaminants [41]. The absence of peaks pertaining to other elements except Bi, Se, O and C ensures the high purity of the product. The high-resolution core spectrum of Bi 4f is shown in Fig. 1 (C), which can be fitted with Bi $4f_{7/2}$ and $4f_{5/2}$ peaks located at 157.6 eV and 162.7 eV respectively [42]. Similarly Fig. 1 (D), shows the high-resolution core spectrum of Se 3d which deconvoluted in to two peaks for Se $3d_{5/2}$ and $3d_{3/2}$ with binding energies of 54.7 and 57.5 eV respectively. Apart from this there is a Selenium oxide (SeO_x) peak observed at 62.1 eV owing to the oxidation of selenium over a prolonged period of time even though the synthesized Bi_2Se_3 was not exposed to air [43].

Fig. 2 (A) shows the SEM image of the layered Bi_2Se_3 - B, while Fig. 2 (B) shows the SEM image of Bi_2Se_3 - FL obtained after exfoliation. From

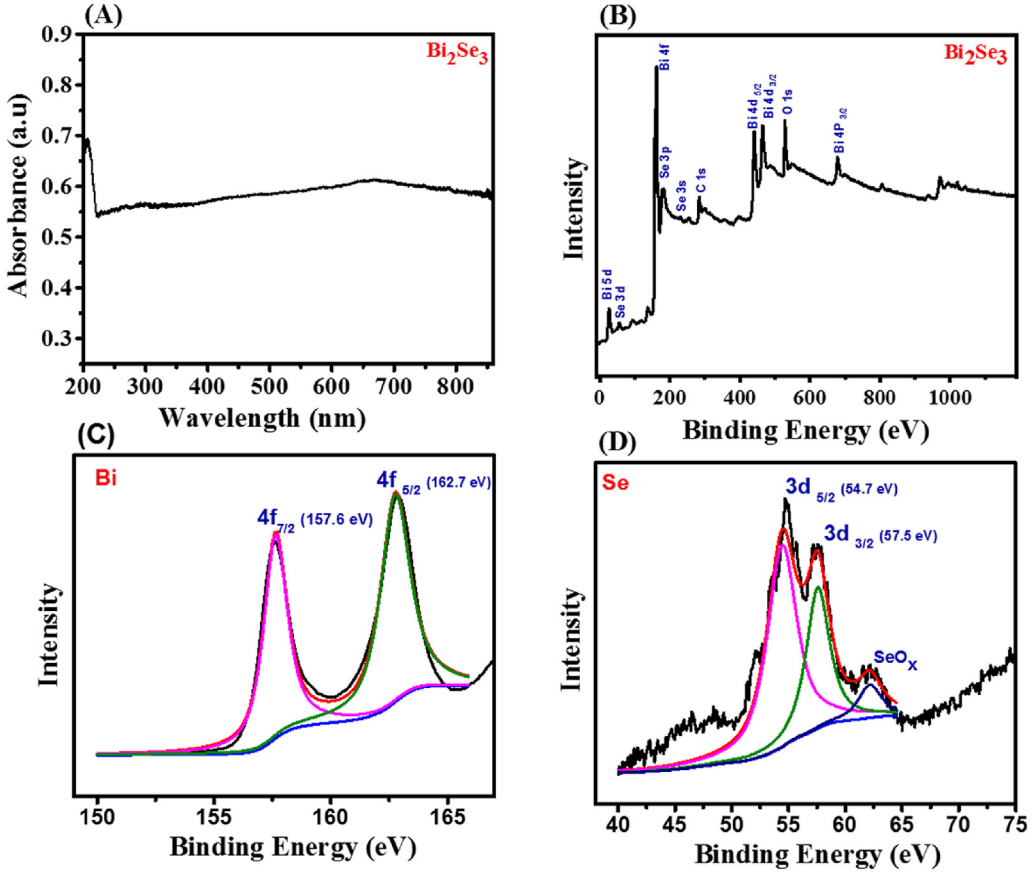

Fig. 1. (A) V-vis absorption spectra of as-synthesized Bi_2Se_3–B; (B) XPS survey scan of Bi_2Se_3–B; Core level XPS spectra of (C) Bi in Bi_2Se_3–B and (D) Se in Bi_2Se_3–B.

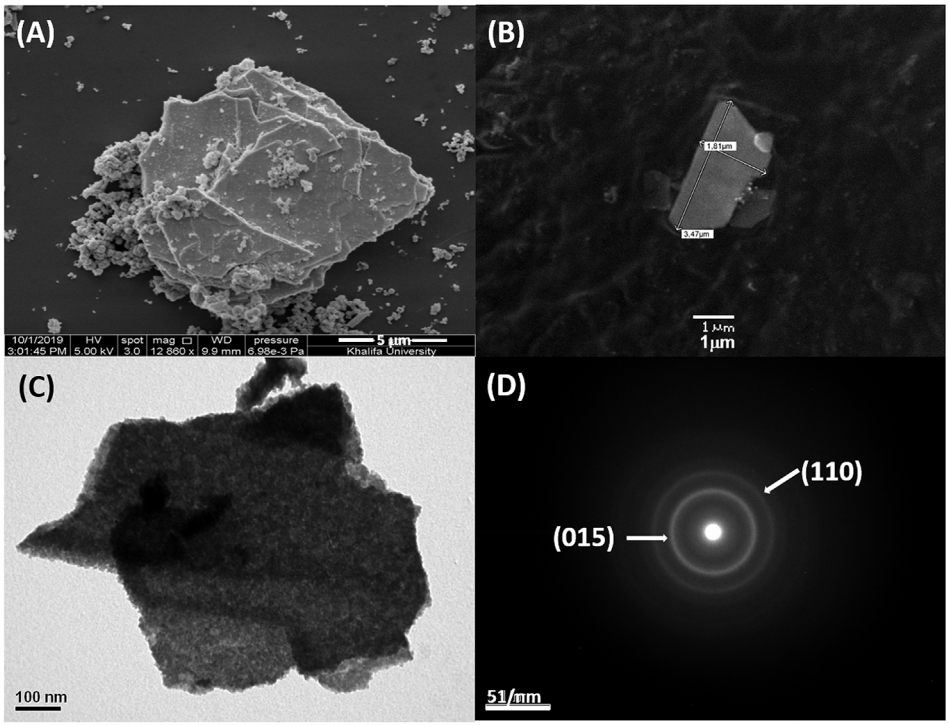

Fig. 2. SEM image of (A) as-synthesized Bi_2Se_3 -B; (B) Bi_2Se_3-FL; (C)TEM image of Bi_2Se_3 - FL and (D) Selected area electron diffraction (SAED).

the SEM images, it can be clearly understood that the synthesized Bi_2Se_3 does possess irregular layered structures and the layers are stacked together. It is also evident that as-synthesized Bi_2Se_3 has mostly layered structures and not particles or rods. The layered structures obtained in this work have been achieved using water as a solvent, without the addition of any surfactant or ionic liquids. The Bi_2Se_3-FL obtained by exfoliation Fig. 2 (B) are found few µm in width, ensuring large surface to volume ratio, which increases the density of free carriers [35]. The EDS analysis and elemental mapping exhibit the presence of Bi and Se in the compound synthesized and their uniform distribution throughout respectively (Fig. S2 (see Supporting information)).

Fig. 2(C) and (D), display TEM micrograph of Bi_2Se_3-FL and its corresponding selected area electron diffraction (SAED) respectively. The TEM image reveals that the exfoliated Bi_2Se_3-FL consist of stacked few layers as compared to Bi_2Se_3–B (Fig. 2(A)).From the TEM images, it is evident that each layer is made up of individual Bi_2Se_3 flakes and the SAED pattern exhibits diffused rings. The diffused rings observed in the electron diffraction indicate the polycrystalline nature of Bi_2Se_3 and they can be indexed to (015) and (110) planes [44,45].The well-defined morphology of the nanostructured Bi_2Se_3 layers is attributed to the uniform "in core" volumetric heating during microwave irradiation with minimized thermal gradients [22–24]. Bi_2Se_3-FL have flake like structure possessing very flat surface with uniform height as seen in the AFM images in Fig. S3(see Supporting information). The thickness of Bi_2Se_3-FL have been measured and it is approximately 10 nm, suggesting that Bi_2Se_3–B has been successfully exfoliated into few layers.

Fig. 3 represents the schematic illustration of the formation of stacked layers of Bi_2Se_3 and exfoliation into few layers. Upon mixing the solution of Na_2SeSO_3 and N_2H_4 with $(Bi(NO_3)_3{\cdot}5H_2O$, the reaction mixture turns dark in color indicating the formation of Bi_2Se_3 flakes at room temperature. The formation of bulk Bi_2Se_3 consisting of individual layers from atomic or molecular scale by chemical reaction follows bottom-up approach [37], whereby microwave irradiation supplies heat energy to the reaction mixture and the individual Bi_2Se_3 flakes move closer to each other and fuse together to form microstructures consisting of few Bi_2Se_3 flakes.

The microstructures thus formed further interact and lead to the formation of large-sized thin layers of Bi_2Se_3.The stacking of the layers proceeds along z-axis through covalent bonding involving five atoms in the order of Se–Bi–Se–Bi–Se and this set of five atoms is called one quintuple layer (QL).The individual 2D Bi_2Se_3 layers are held together by weak van der Waals forces giving rise to stacked layers of 3D layered structure [37].The bulk 3D stacked layers are to be subjected to exfoliation in order to get 2D single - layer or few-layer Bi_2Se_3 by top-down approach as in the case of graphene. Bi_2Se_3-FLwere obtained through sonication assisted liquid-phase exfoliation. During sonication, the mechanical force from sonication is strong enough to overcome the weak van der Waals forces holding the individual Bi_2Se_3 layers, giving way for exfoliation. Each layer of Bi_2Se_3 is made up of several individual Bi_2Se_3 flakes and these exfoliated few - layers possess high surface area to volume ratio, which is advantageous over the bulk 3D material in terms enhanced catalytic activity.

3.2. Electrochemical applications

In this section, inherent electrochemical and the catalytic properties of the nanostructured Bi_2Se_3-FL are discussed via non-enzymatic glucose sensing.

Fig. 4(A and B) depict the cyclic voltammograms (CVs) recorded for bare glassy carbon (GC) electrode (a) and Bi_2Se_3-FLmodified GC electrode(b) in the absence (A) and in the presence (B) of $K_3[Fe(CN)_6]$ in 0.1 M KCl at a scan rate of 0.05 Vs^{-1}. The Bi_2Se_3-FL/G C electrode (Fig. 4 (A) curve (b)) shows higher current than the bare GC (Fig. 4(A) curve (a)), owing to the existence of electroactive species (Bi_2Se_3 -FL) on the electrode surface. The cyclic voltammograms recorded for the $[Fe(CN)6]^{3-/4-}$couple for bare GC (Fig. 4 (B) curve (a)) and Bi_2Se_3-FL modified GC (Fig. 4 (B) curve (b))in 0.1 M KCl solution exhibits a reversible electrochemical response for the $[Fe(CN)6]^{3-/4-}$ couple (Fig. 4(B) curve (a)), the difference between the redox potential (ΔEp) of the bare GC electrode in the PBS solution of $[Fe(CN)6]^{3-/4-}$ is found to be 70 mV, and the fine peak representing that the bare electrode has excellent conductivity. On introducing Bi_2Se_3-FL over the surface of GC electrode the peak current is found to increase. Therefore, it is evident that the Bi_2Se_3-FL/GC stands out to be superior to bare GC, in terms of electron transfer, that can be

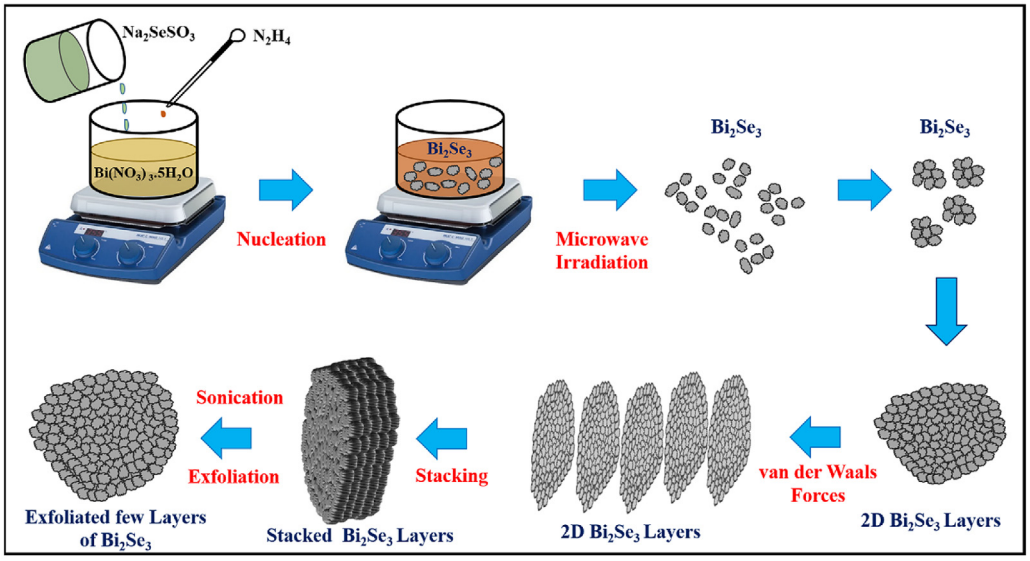

Fig. 3. Schematic illustration of the formation of stacked layers of Bi_2Se_3 and exfoliation Process.

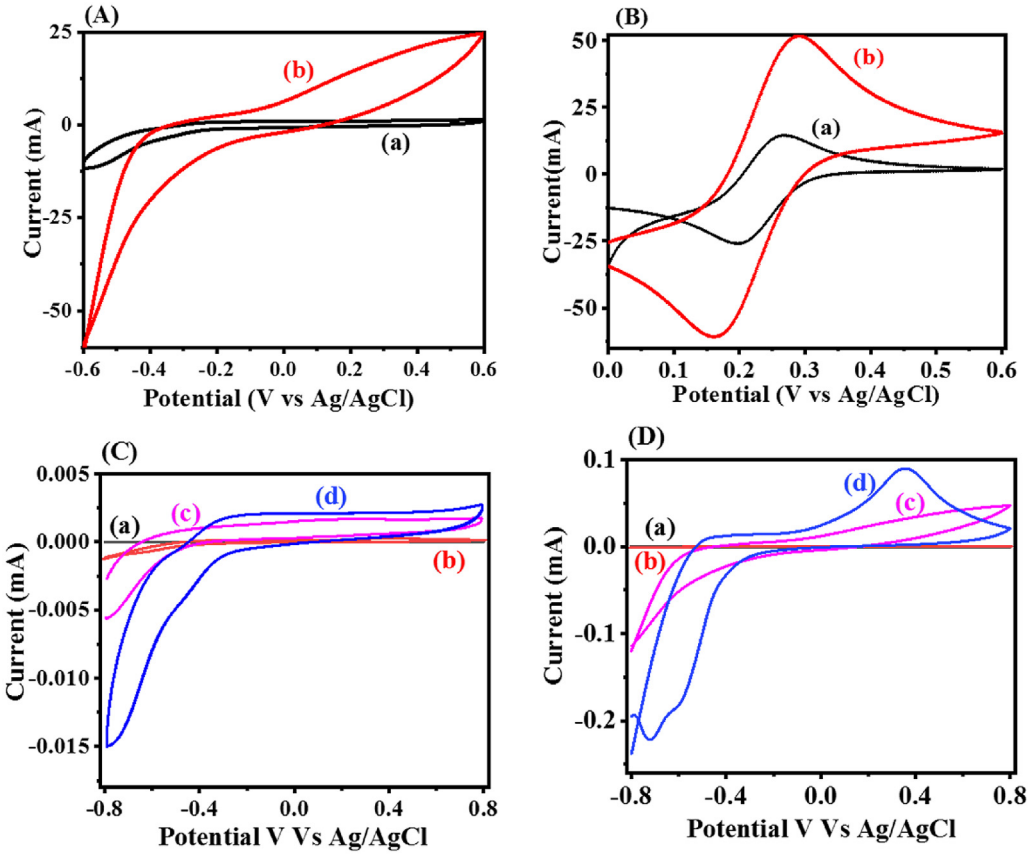

Fig. 4. Cyclic voltammograms recorded for (A) in the absence and (B) the presence of 5×10^{-3} $M[Fe(CN)_6]^{3-/4-}$ in 0.1 M KCl solution recorded for (a) BareGC and (b) Bi_2Se_3-FL/GC electrode; (C) bare GC (a and b) and Bi_2Se_3–Bulk/GC (c and d) in 0.1 M PBS (pH 7.0) in the absence (a and c) and presence (b and d) of 10 mM glucose; (D) bare GC (a and b) and Bi_2Se_3–FL/GC (c and d) in 0.1 M PBS (pH 7.0) in the absence (a and c) and in the presence (b and d) of 10 mM glucose under the optimal experimental conditions. Scan rate: $0.05 Vs^{-1}$.

attributed to the electrochemically active sites on the surface of Bi_2Se_3 layers which assist the electron transfer process and the high specific area of the Bi_2Se_3-FL. Additionally, the peak separation (ΔEp) is found to be large for Bi_2Se_3-FL modified GC (125 mV) as compared to bare GC (70 mV), signifying that the electrochemical redox potential in electrode is quasi reversible. This behavior suggest that Bi_2Se_3-FLsurface is negatively charged, which is due to the electrostatic repulsion between ferricyanide and surface of Bi_2Se_3-FL [46].

3.2.1. *Electrocatalytic oxidation of glucose at the Bi_2Se_3/GC*

The electrochemical behavior of Bi_2Se_3-FL/GC towards glucose sensor was examined by cyclic voltammetry technique in a potential ranging from −0.8 to +0.8 V at scan rate 0.05 Vs^{-1} and compared it with Bi_2Se_3–B/GC. Fig. 4 (C) displays the CVs of the bare GC electrode ((a) and (b)) and Bi_2Se_3–B/GC ((c) and (d)) in 0.1 M PBS (pH 7.0) solution in the absence ((a) and (c)) and in the presence ((b) and (d)) of 10 mM glucose. Similarly Fig. 4 (D) shows the CVs of the bare GC ((a) and (b)) are

compared with that of Bi_2Se_3-FL/GC ((c) and(d)) in the absence ((a) and (c)) and in the presence ((b) and (d)) of 10 mM glucose in 0.1 M PBS (pH 7.0) solution For the bare GC no significant peak is observed in CV both in the presence and absence of 10 mM glucose (curves (a)and (b) in Fig. 4(C) and (D)) in the 0.1 M PBS (pH 7.0). In both the cases, bare GC demonstrated low electrochemical performance than Bi_2Se_3-FL/GC and Bi_2Se_3–B/GC. The comparison of the CV performance of the Bi_2Se_3–B/GC (Fig. 4 (C), curve (a)) with Bi_2Se_3-FL/GC (Fig. 4(D), curve (c)), in the absence of the glucose, revealed Bi_2Se_3-FL/GC electrode had a superior performance over Bi_2Se_3–B/GC electrode by exhibiting a very sharp peak with current of 9.25×10^{-4} A in the presence of glucose (d) which is ~3 and 9 times higher than that of the Bi_2Se_3-FL modified GC in the absence of glucose (Fig. 4 (D) curve (c)) and the bare GC in the presence of glucose (Fig. 4 (D curve (b)), respectively. The high peak potential exhibited by the Bi_2Se_3-FL/GC electrode evidences for the well-defined electrocatalytic feature of the Bi_2Se_3 to direct oxidation of the glucose in the PBS solution. Therefore, Bi_2Se_3-FL/GC is chosen for the sensing application over Bi_2Se_3–B/GC while bare GC was retained for comparison.

Fig. 5, (A) presents the results of the typical linear sweep voltammetry (LSV) obtained for both bare GC (a) and Bi_2Se_3-FL/GC (b) in 0.1 M PBS (pH 7.0) solution with 10 mM of glucose addition at a scan rate of 0.05Vs^{-1}. It can be seen that the bare GC does not show any oxidation peak current in the presence of glucose (curve (a)), indicating its negligible electrochemical activity for glucose oxidation. On the contrary, Bi_2Se_3-FL/GC demonstrates a strong oxidation peak (curve (b)) at 0.28V and 1.5 μA even in the absence of glucose and a very sharp higher oxidation peak current (4×10^{-4} A) with lower oxidation potential (0.19 V) (curve (c)), after adding 1 mM glucose evidences for better electrocatalytic activity of the Bi_2Se_3-FL towards glucose solutions in comparison to bare GC. From the Electrochemical Impedance Spectroscopy (EIS) it is evident that electro-transfer resistance of Bi_2Se_3-FL/GC electrode is significantly less than that of the bare GC implying that the former can play better role in electrocatalysis than the latter, which is evident from its electrochemical oxidation of glucose (Fig. 5 (B)). The charge transfer resistance (Rct) of the bare GC is 165 Ω, however, after modifying with Bi_2Se_3 -FL the electrode's Rct value decreases to 114 Ω, suggesting that Bi_2Se_3 - FL is a better medium for electron transfer.

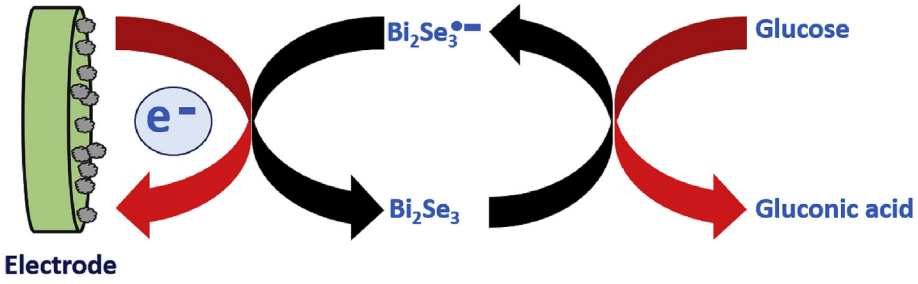

(1)

In general, Bi_2Se_3 behaves as an n-type semiconductor due to the charged selenium vacancies which are lattice defects but acting as electron donors [47–49]. The set of five monoatomic layers where the atoms are covalently bonded in the order Se–Bi–Se–Bi–Se, has Se on either side making it almost like a bidentate ligand [18]. During the electrochemical process, Bi_2Se_3 is converted to $Bi_2Se_3^{\bullet-}$species by one electron trapping process occurring on the surface of Bi_2Se_3 at 0.41 V, which is regenerated upon oxidation at −0.60V. When glucose approaches the surface of $Bi_2Se_3^{\bullet-}$ radical anion it reduces $Bi_2Se_3^{\bullet-}$to Bi_2Se_3 and glucose gets oxidized in the process. Therefore, Bi_2Se_3 acts as effective electrocatalyst to oxidize glucose and the extent of glucose oxidation is proportional to the current produced. Here Bi_2Se_3 functions as a mediator to enhance the electron transfer between the electrode and glucose and the electrochemical detection of glucose by using $Bi_2Se_3$is illustrated by the following equation (1) [50,51].

Fig. 6 (A) exhibits the modified Bi_2Se_3-FL/GC electrode's reaction kinetics examination by recording the influence of different scan rates (υ) while oxidizing glucose. As it is seen in Fig. 6(A), the oxidation peak current increases with the increase in υ value and there is a good linear relationship between the current (i_p) and υ. The plotted relationship verifies that i_p response is linearly proportional to square root of scan rate ranging between 0.01 Vs^{-1} and 0.15 Vs^{-1}(see Fig. 6(B)). The linear

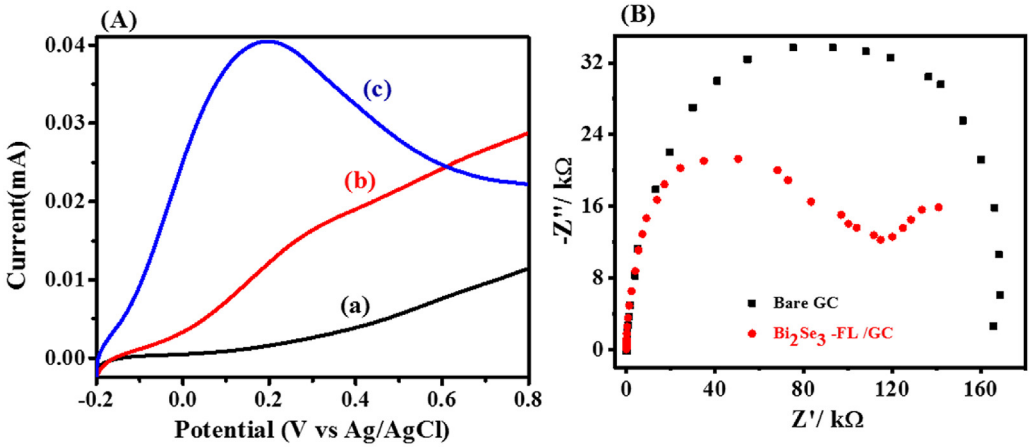

Fig. 5. (A) LSV curves of bare GC (a) and Bi_2Se_3-FL/GC (b and c) in 0.1 M PBS (pH 7.0) in the presence of 10 mM glucose (a and c) and in the absence of glucose (b), under the optimal experimental conditions; (B) Electrochemical impedance spectrum for bare GC and Bi_2Se_3-FL/GC 1.0 mM $[Fe(CN)_6]^{3-/4-}$ in 0.1 M KCl.

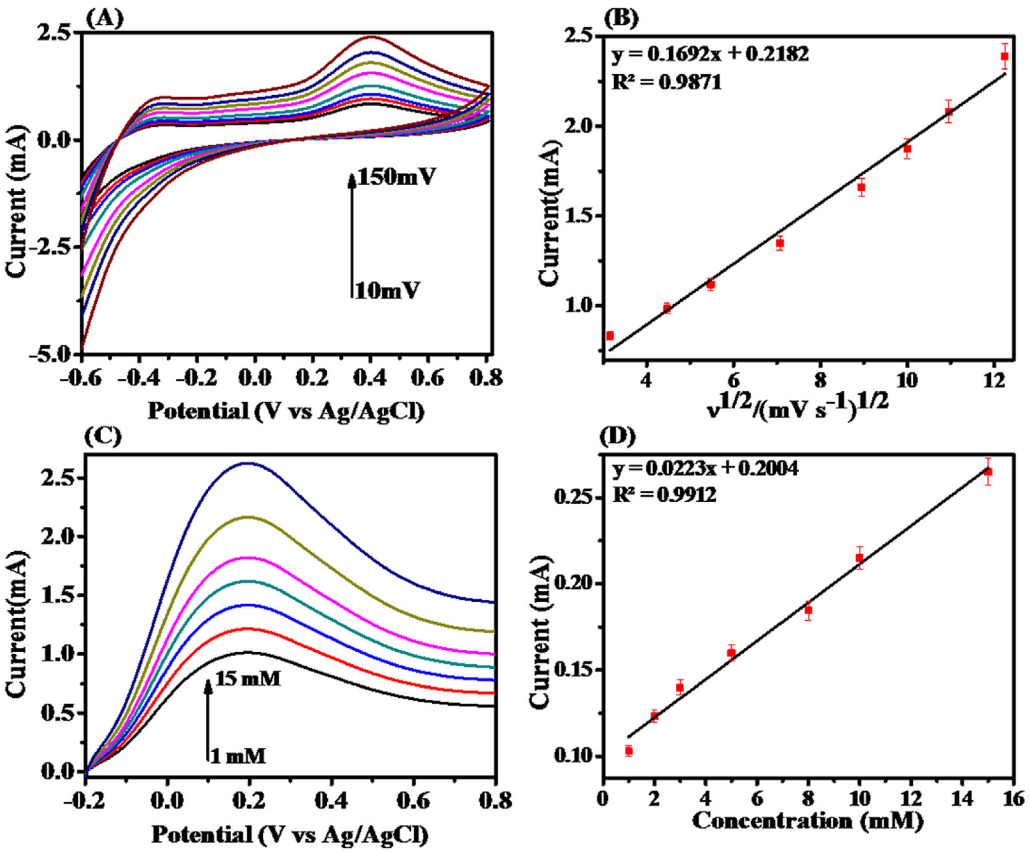

Fig. 6. (A) Cyclic voltammetry curves for Bi_2Se_3-FL/GC in 1 mM glucose (scan rate 10, 20,30, 50, 80, 100, 120 and 150 mVs^{-1}); (B) plot of peak current (i_p) vs. square root of scan rate ; (C) LSV of Bi_2Se_3-FL/GC electrode with different glucose concentrations: 10, 20, 30, 50,80, 100 and 150 μM (0.1 M PBS (pH 7.0), scan rate: 0.05 Vs−1); (D) calibration plot of current vs concentration.

relationship between the current vs square root of scan rate represents that it is a diffusion controlled processes ($I_{pa}/\mu A = 0.1692$ mA$(mVs^{-1})^{1/2}$+ 0.2182 mA, $R^2 = 0.9871$). The above consequences specify that the sensor constructed is very stable and a highly reliable electrochemical sensing platform.

As a rapid and appropriate technique for illustrating glucose sensors [52], LSV is employed to explore the electrocatalytic activity of Bi_2Se_3-FL/GC on oxidizing glucose. The LSV of Bi_2Se_3/GC in the presence of different concentrations of glucose in PBS at a scan rate of 0.05 V $s^{-1}$is carried out (Fig. 6 (C)). After adding a definite amount of glucose to PBS, a notable anodic peak is accomplished at about 0.19 V. This oxidation peak is due to glucose oxidation and it is confirmed by the addition of different concentrations of glucose. When glucose is added to the PBS solution, the oxidation peak current enormously increases as the concentration of glucose is increased from 1 to 15 mM over a potential range of −0.2 - +0.8 V reaching a peak value of +0.19 V in 0.1 M PBS solution. Upon the addition of glucose, the oxidation peak current increases linearly. From the calibration plot (Fig. 6 (D)) of current vs concentration, it is clearly seen that there is a linear detection range of 15 mM, while the detection sensitivity is 0.022 mA $mM^{-1}$with a correlation coefficient (R^2) of 0.9912.The obtained oxidation peak current signals show the important catalytic activity of Bi_2Se_3-FL/GC in its response to glucose. This demonstrates that the Bi_2Se_3-FL/GC is a promising candidate in improving the analytical ability of sensing glucose.

Fig. 7 (A) shows the amperometric response of bare GC (a) and Bi_2Se_3-FL/GC (b) at 0.19 V with successive additions of glucose into 0.1 M PBS (pH 7.0) solution at constant intervals. The electrode displays a quick response when glucose is added, and the time to attain 96% steady-state current is not more than 3s, representing a very rapid and good response for glucose. The corresponding calibrationplots for the electrodes over the glucose concentration range of 10–100 μM are presented in Fig. 7(B).

The current response has linearly increased on increasing glucose concentration, as shown in the calibration plot (current vs glucose concentration) of amperometric response in Fig. 7 (B). The calibration plot is found to be linear with a correlation coefficient (R^2) of 0.9921. The regression equation y = 0.112*x* - 0.071 with the lower detection limit (LOD) is observed to be as low as 6.1 μM at the signal-to-noise ratio (S/N) of 3. Additional, sensitivity is calculated as 0.112 μAμM^{-1} by dividing the slope of the linear portion of calibration plots with electrode surface area. The improved sensing performance of non-enzymatic glucose sensor attributed to Bi_2Se_3-FL/GC electrode is because it offers high surface area, resulting in rapid electron transfer through electrochemical process for the oxidation of glucose occurring between the electrolyte and electrode.The results obtained here evidence the feasibility to fabricate Bi_2Se_3-FL based non-enzymatic glucose sensor with sufficient stability, sensitivity, selectivity and with good reproducibility. To support our claim further we have compared this work with other recently published works on non-enzymatic glucose senors and presented in Table S1(see supplementary information). [S1-S8].

3.2.2. Interference analysis, repeatability and reproducibility of the Bi_2Se_3-FL/GC modified electrode

In addition to sensitivity, selectivity and anti-interference are the other significant features expected of high-performance non-enzymatic glucose biosensors as poor selectivity and interference of other species can bring down the performance of the device. Hence sensitivity and anti-interference capacity of the Bi_2Se_3-FL/GC electrode was evaluated and presented here. Fig. 8 shows, the selectivity of Bi_2Se_3-FL/GC electrode toward glucose sensing in the presence of different interfering species such as ascorbic acid (AA), dopamine (UA), uric acid (DA), and sucrose. The detection is demonstrated using the amperometric response of the electrode sensing with the adding of 2 μM glucose and 2 μM of each

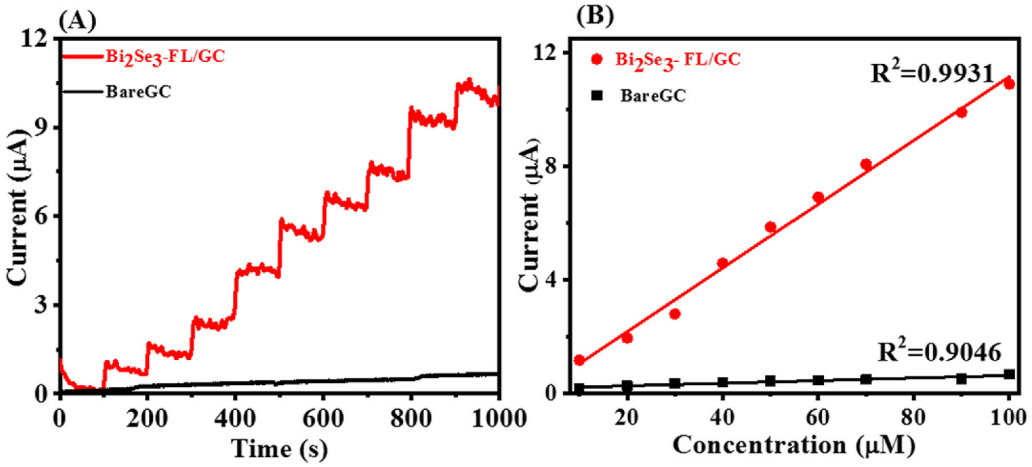

Fig. 7. (A) Amperometric current–time (i–t) curves to the successive addition of glucose in 0.1 M PBS (pH 7.0) at constant potential: 0.19 V. (B) The corresponding calibration curve current versus concentration of glucose.

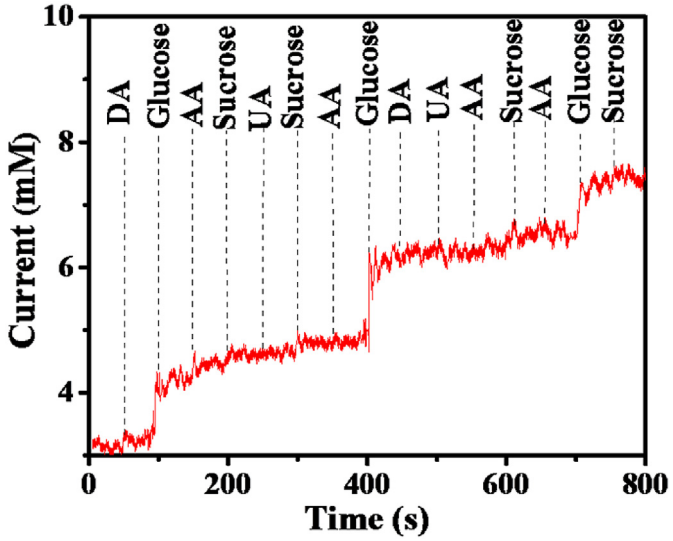

Fig. 8. Amperometric responses of Bi_2Se_3-FL/GC to successive additions of 2.0 μM glucose and 1.0 μM UA, AA, DA and Sucrose in 0.1 M PBS (pH 7.0) at 0.19 V.

of the above interfering analytes in a solution of PBS (0.1 M) at +0.19 V (vs Ag/AgCl).It can be seen that, after each addition of glucose the current response raises; whereas when interfering analytes are added negligible current responses are observed. The above results suggest that the fabricated Bi_2Se_3-FL/GC electrode can be used for selective detection of glucose and also for the determination of glucose in real samples under physiological conditions.

The stability of the Bi_2Se_3-FL/GC sensor is observed by analyzing its response of current to glucose over 19 days. After 19 days, only 17% loss in current signal is detected from its initial response (see Figs. S4(A) and S4(B) in supplementary information). The excellent stability of modified electrode can be ascribed to the stability of Bi_2Se_3- FL. To examine the reproducibility of the Bi_2Se_3-FL/GC sensor towards the electrocatalytic oxidation of glucose, five freshly prepared electrodes were assessed by associating their current responses in 0.1 M PBS containing 10 mM glucose at the scan rate of 50 mVs^{-1} (Fig. S4(C) and S4 (D) in supplementary information).A relative standard deviation (RSD) of 2.4% is obtained, indicating the reliability of the method and material. A set of 5 measurements for a distinct electrode was made upon the addition of 10 mM glucose in 0.1 M PBS, and it resulted in 3.1% of RSD, demonstrating excellent reproducibility. Likewise, the repeatability Bi_2Se_3-FL/GC electrode is measured using 6 models separately, by adding 10 mM of glucose at 50 mVs^{-1}scan rate (see Figs. S4(E) and S4 (F) in supplementary information).After 6 times usage, Bi_2Se_3-FL/GC glucose sensing electrode retained around 94% of its original response, exhibiting outstanding reproducibility and repeatability of non-enzymatic glucose sensing ability.

3.2.3. *Real sample analysis*

The outstanding detecting performance of Bi_2Se_3-FL/GC electrode suggests its appropriateness for glucose detection in real samples, which was examined by detecting the glucose present in the urine sample collected from a healthy volunteer. The human participants were informed of the consents.The glucose concentration was detected at the Bi_2Se_3-FL/GC in the presence of 100 μL of urine. For all the tests, standard glucose was added to calculate the recovery rate, and the Bi_2Se_3-FL/GC sensor displayed a good recovery in between 96.0 and 101.2%, with a fine RSD value of 2.3% (n = 3) [53,54].These results obtained strongly suggest that the Bi_2Se_3-FL/GC has noticeable potential application in repetitive glucose sensing, with promising precision and accuracy Table S2(see supplementary information).

4. Conclusion

In summary, we have successfully developed Bi_2Se_3- FL based non-enzymatic electrochemical glucose sensor. The individual Bi_2Se_3 layers are made up of small Bi_2Se_3 flakes which result in larger surface area and exhibit Localized Surface Plasmon Resonance (LSRP) because of cation vacancy exhibited enhanced electrocatalytic activity. The experimental results obtained demonstrated that Bi_2Se_3-FL/GC electrodes possess excellent electrocatalytic activity towards the oxidation of glucose and upon glucose addition, the system reached steady-state level within 3 s. The interface showed a linear behavior from 10 μM to 100 μM of glucose concentration, with a current sensitivity of 0.112 $\mu A \mu M^{-1}$ and a detection limit of 6.1 μM. The Bi_2Se_3 - FL based glucose sensors exhibited fast response, high sensitivity and good stability towards the oxidation of glucose. All these results suggest that the proposed sensor is an attractive and effective tool for practical glucose monitoring and opens a new avenue to explore the potential applications of Bi_2Se_3 in the field of electrochemical biosensors/sensors.

Acknowledgments

The authors A.Dennyson Savariraj and R.V.Mangalaraja gratefully acknowledge the FONDECYT Post-doctoral Project No. 3170640, Government of Chile, Santiago, for the financial assistance. The authors wish

to thank Julio Pugin Rios, Ricardo Oliva Carrasco, Alexis Estay Valencia and Monica Del Carmen Uribe Sazo in the microscopy facility at the University of Concepcion for their kind cooperation.

Appendix A. Supplementary data

Supplementary data to this article can be found online at https://doi.org/10.1016/j.jelechem.2019.113629.

References

[1] T. Chen, D. Liu, W. Lu, K. Wang, G. Du, A.M. Asiri, et al., Three-dimensional Ni2P nanoarray: an efficient catalyst electrode for sensitive and selective nonenzymatic glucose sensing with high specificity, Anal. Chem. 88 (2016) 7885–7889.

[2] S. Park, H. Boo, T.D. Chung, Electrochemical non-enzymatic glucose sensors, Anal. Chim. Acta 556 (2006) 46–57.

[3] L.C. Clark Jr., C. Lyons, Electrode systems for continuous monitoring in cardiovascular surgery, Ann. N. Y. Acad. Sci. 102 (1962) 29–45.

[4] C. Zhang, Z. Zhang, Q. Yang, W. Chen, Graphene-based electrochemical glucose sensors: fabrication and sensing properties, Electroanalysis 30 (2018) 2504–2524.

[5] F. Xie, T. Liu, L. Xie, X. Sun, Y. Luo, Metallic nickel nitride nanosheet: an efficient catalyst electrode for sensitive and selective non-enzymatic glucose sensing, Sens. Actuators B Chem. 255 (2018) 2794–2799.

[6] J. Huang, Y. He, J. Jin, Y. Li, Z. Dong, R. Li, A novel glucose Sensor Based on MoS_2 nanosheet functionalized with Ni nanoparticles, Electrochim. Acta 136 (2014) 41–46.

[7] L. Xie, A.M. Asiri, X. Sun, Monolithically integrated copper phosphide nanowire: an efficient electrocatalyst for sensitive and selective nonenzymatic glucose detection, Sens. Actuators B Chem. 244 (2017) 11–16.

[8] B. Zhou, Y. Zhao, L. Pu, J. Zhu, Microwave-assisted synthesis of nanocrystalline Bi_2Te_3, Mater. Chem. Phys. 96 (2006) 192–196.

[9] Y. Jiang, Y. Zhu, G. Cheng, Synthesis of Bi2Se3 nanosheets by microwave heating using an ionic liquid, Cryst. Growth Des. 6 (2006) 2174–2176.

[10] P. Larson, V.A. Greanya, W.C. Tonjes, R. Liu, S.D. Mahanti, C.G. Olson, Electronic structure of Bi_2X_3 (S=S,Se,Te)compounds: comparison of theoretical calculations with photoemission studies, Phys. Rev. B 65 (2002), 085108.

[11] S. Urazhdin, D. Bilc, S.H. Tessmer, S.D. Mahanti, T. Kyratsi, M.G. Kanatzidis, Scanning tunneling microscopy of defect states in the semiconductor Bi_2Se_3, Phys. Rev. B 66 (2002) 161306.

[12] Q. Wang, G. Chen, D. Chen, R. Jin, Amine-assisted solution approach for the synthesis and growth mechanism of super-long rough-surfaced Cu_7Te_4 nanobelts, CrystEngComm 14 (2012) 6962–6973.

[13] X. Qiu, J. Zhu, L. Pu, Y. Shi, Y. Zheng, H. Chen, Size-controllable sonochemical synthesis of thermoelectric material of Bi_2Se_3 nanocrystals, Inorg. Chem. Commun. 7 (2004) 319–321.

[14] J. Waters, D. Crouch, J. Raftery, P. O'Brien, Deposition of bismuth chalcogenide thin films using novel single-source precursors by metal-organic chemical vapor deposition, Chem. Mater. 16 (2004) 3289–3298.

[15] P. Kumar, P. Srivastava, J. Singh, R. Belwal, M.K. Pandey, K.S. Hui, et al., Morphological evolution and structural characterization of bismuth telluride (Bi_2Te_3) nanostructures, J. Phys. D 46 (2013) 285301.

[16] H. Liu, H. Cui, F. Han, X. Li, J. Wang, R.I. Boughton, Growth of Bi_2Se_3 nanobelts synthesized through a Co-reduction method under ultrasonic irradiation at room temperature, Cryst. Growth Des. 5 (2005) 1711–1714.

[17] X. Qiu, C. Burda, R. Fu, L. Pu, H. Chen, J. Zhu, Heterostructured Bi_2Se_3 nanowires with periodic phase boundaries, J. Am. Chem. Soc. 126 (2004) 16276–16277.

[18] A. Ambrosi, Z. Sofer, J. Luxa, M. Pumera, Exfoliation of layered topological insulators Bi_2Se_3 and Bi_2Te_3 via electrochemistry, ACS Nano 10 (2016) 11442–11448.

[19] G. Shen, D. Chen, K. Tang, Y. Qian, Self-sacrificing template route to novel patterns of radially aligned $Bi_2(Se,S)_3$ nanorods and Bi_2Se_3 flakes, Nanotechnology 15 (2004) 1530–1534.

[20] J.J.J. Vijila, K. Mohanraj, J. Henry, G. Sivakumar, Microwave-assisted Bi_2Se_3 nanoparticles using various organic solvents, Spectrochim. Acta A Mol. Biomol. Spectrosc. 153 (2016) 457–464.

[21] M. Baghbanzadeh, L. Carbone, P.D. Cozzoli, C.O. Kappe, Microwave-assisted synthesis of colloidal inorganic nanocrystals, Angew. Chem. Int. Ed. 50 (2011) 11312–11359.

[22] I. Bilecka, M. Niederberger, Microwave chemistry for inorganic nanomaterials synthesis, Nanoscale 2 (2010) 1358–1374.

[23] Y. He, L. Sai, H. Lu, M. Hu, W. Lai, Q. Fan, et al., Microwave-assisted synthesis of water-dispersed CdTe nanocrystals with high luminescent efficiency and narrow size distribution, Chem. Mater. 19 (2007) 359–365.

[24] I. Bilecka, P. Elser, M. Niederberger, Kinetic and thermodynamic aspects in the microwave-assisted synthesis of ZnO nanoparticles in benzyl alcohol, ACS Nano 3 (2009) 467–477.

[25] R. Hoogenboom, U.S. Schubert, Microwave-assisted polymer synthesis: recent developments in a rapidly expanding field of research, Macromol. Rapid Commun. 28 (2007) 368–386.

[26] B. Temur Ergan, M. Bayramoglu, Kinetic approach for investigating the "microwave effect": decomposition of aqueous Potassium persulfate, Ind. Eng. Chem. Res. 50 (2011) 6629–6637.

[27] A.Y. Nikitin, F. Guinea, F. Garcia-Vidal, L. Martin-Moreno, Surface plasmon enhanced absorption and suppressed transmission in periodic arrays of graphene ribbons, Phys. Rev. B 85 (2012), 081405.

[28] P.K. Jain, Plasmon-in-a-Box: on the physical nature of few-carrier plasmon resonances, J. Phys. Chem. Lett. 5 (2014) 3112–3119.

[29] P.K. Jain, X. Huang, I. El-Sayed, M. El-Sayed, Review of some interesting surface plasmon resonance-enhanced properties of noble metal nanoparticles and their applications to biosystems, Plasmonics 2 (2007) 107–118.

[30] A. Soni, Z. Yanyuan, Y. Ligen, M.K.K. Aik, M.S. Dresselhaus, Q. Xiong, Enhanced thermoelectric properties of solution grown $Bi_2Te_{3-x}Se_x$ nanoplatelet composites, Nano Lett. 12 (2012) 1203–1209.

[31] F. Xie, X. Cao, F. Qu, A.M. Asiri, X. Sun, Cobalt nitride nanowire array as an efficient electrochemical sensor for glucose and H_2O_2 detection, Sens. Actuators B Chem. 255 (2018) 1254–1261.

[32] Z. Wang, X. Cao, D. Liu, S. Hao, R. Kong, G. Du, et al., Copper-nitride nanowires array: an efficient dual-functional catalyst electrode for sensitive and selective non-enzymatic glucose and hydrogen peroxide sensing, Chem. Eur J. 23 (2017) 4986–4989.

[33] D. Zhou, X. Cao, Z. Wang, S. Hao, X. Hou, F. Qu, et al., Fe_3N-Co_2N nanowires array: a non-noble-metal bifunctional catalyst electrode for high-performance glucose oxidation and H_2O_2 reduction toward non-enzymatic sensing applications, Chem. Eur J. 23 (2017) 5214–5218.

[34] A.D. Savariraj, G. Rajendrakumar, S. Selvam, S.N. Karthick, B. Balamuralitharan, H. Kim, et al., Stacked $Cu_{1.8}S$ nanoplatelets as counter electrode for quantum dot-sensitized solar cell, RSC Adv. 5 (2015) 100560–100567.

[35] J. Guozhi, W. Peng, Z. Yanbang, C. Kai, Localized surface plasmon enhanced photothermal conversion in Bi_2Se_3 topological insulator nanoflowers, Sci. Rep. 6 (2016) 25884.

[36] Y. Min, G.D. Moon, B.S. Kim, B. Lim, J. Kim, C.Y. Kang, et al., Quick, controlled synthesis of ultrathin Bi_2Se_3 nanodiscs and nanosheets, J. Am. Chem. Soc. 134 (2012) 2872–2875.

[37] L. Sun, Z. Lin, J. Peng, J. Weng, Y. Huang, Z. Luo, Preparation of few-layer bismuth selenide by liquid-phase-exfoliation and its optical absorption properties, Sci. Rep. 4 (2014) 4794.

[38] J.M. Luther, P.K. Jain, T. Ewers, A.P. Alivisatos, Localized surface plasmon resonances arising from free carriers in doped quantum dots, Nat. Mater. 10 (2011) 361–366.

[39] A. Dennyson Savariraj, H. Kim, S. Karuppanan, K. Prabakar, Phase transformation and evolution of localized surface plasmon resonance in $Cu_{2-x}S$ thin films deposited at 60°C, J. Phys. Chem. C 121 (2017) 25440–25446.

[40] A.D. Savariraj, K.K. Viswanathan, K. Prabakar, Influence of Cu vacancy on knit coir mat structured CuS as counter electrode for quantum dot sensitized solar cells, ACS Appl. Mater. Interfaces 6 (2014) 19702–19709.

[41] P.H. Le, K.H. Wu, C.W. Luo, J. Leu, Growth and characterization of topological insulator Bi_2Se_3Thin films on $SrTiO_3$ using pulsed laser deposition, Thin Solid Films 534 (2013) 659–665.

[42] K. Zhang, H. Pan, Z. Wei, M. Zhang, F. Song, X. Wang, et al., Synthesis and magnetotransport properties of Bi_2Se_3 nanowires, Chin. Phys. B 26 (2017), 096101.

[43] D. Kong, J.J. Cha, K. Lai, H. Peng, J.G. Analytis, S. Meister, et al., Rapid surface oxidation as a source of surface degradation factor for Bi_2Se_3, ACS Nano 5 (2011) 4698–4703.

[44] D. Li, M. Fang, C. Jiang, H. Lin, C. Luo, R. Qi, et al., Size-controlled synthesis of hierarchical bismuth selenide nanoflowers and Their photocatalytic performance in the presence of H_2O_2, J. Nanoparticle Res. 20 (2018) 228.

[45] P. Sahu, J. Chen, J.C. Myers, J. Wang, Weak antilocalization and low-temperature characterization of sputtered polycrystalline bismuth selenide, Appl. Phys. Lett. 112 (2018) 122402.

[46] B.G. Mahmoud, M. Khairy, F.A. Rashwan, C.W. Foster, C.E. Banks, Self-assembly of porous copper oxide hierarchical nanostructures for selective determinations of glucose and ascorbic acid, RSC Adv. 6 (2016) 14474–14482.

[47] K. Mazumder, A. Sharma, Y. Kumar, P.M. Shirage, Effect of Cu intercalation on humidity sensing properties of Bi2Se3 topological insulator single crystals, Phys. Chem. Chem. Phys. 20 (2018) 28257–28266.

[48] M.Z. Hasan, C.L. Kane, Colloquium: topological insulators, Rev. Mod. Phys. 82 (2010) 3045–3067.

[49] J. Navratil, J. Horak, T. Plechacek, S. Kamba, P. Lostak, J.S. Dyck, et al., Conduction band splitting and transport properties of Bi_2Se_3, J. Solid State Chem. 177 (2004) 1704–1712.

[50] A.K. Dutta, S.K. Maji, K. Mitra, A. Sarkar, N. Saha, A.B. Ghosh, et al., Single source precursor approach to the synthesis of Bi_2S_3 nanoparticles: a new amperometric hydrogen peroxide biosensor, Sens. Actuators B Chem. 192 (2014) 578–585.

[51] G. Zhao, J. Feng, Q. Zhang, S. Li, H. Chen, Synthesis and characterization of prussian blue modified magnetite nanoparticles and its application to the electrocatalytic reduction of H_2O_2, Chem. Mater. 17 (2005) 3154–3159.

[52] R. Zhao, X. Liu, J. Zhang, J. Zhu, D.K.Y. Wong, Enhancing direct electron transfer of glucose oxidase using a gold nanoparticle titanate nanotube nanocomposite on a biosensor, Electrochim. Acta 163 (2015) 64–70.

[53] S. Ata, F.H. Wattoo, M. Ahmed, M.H.S. Wattoo, S.A. Tirmizi, A. Wadood, A method optimization study for atomic absorption spectrophotometric determination of total zinc in insulin using direct aspiration technique, Alexandria Journal of Medicine 51 (2015) 19–23.

[54] B. Arshad, T. Iqbal, S. Akram, M. Mushtaq, An expedient reverse-phase high-performance chromatography (RP-HPLC) based method for high-throughput analysis of deferoxamine and ferrioxamine in urine, Biomed. Chromatogr. 31 (2017), e3805.